Global J. Environ. Sci. Manage. 6(2): 215-232, Spring 2020

Global Journal of Environmental Science and Management
(GJESM)

Homepage: https://www.gjesm.net/

ORIGINAL RESEARCH PAPER

Simulation and prediction of land use and land cover change using GIS, remote sensing and CA-Markov model

H.A. Khawaldah*, I. Farhan, N.M. Alzboun

Department of Geography, Faculty of Arts, The University of Jordan, Amman, Jordan

ARTICLE INFO

Article History:
Received 17 August 2019
Revised 25 November 2019
Accepted 07 December 2019

Keywords:
CA-Markov model
Jordan
Land use/land cover change (LULC)
Population growth
Urban expansion

ABSTRACT

This study analyzes the characteristics of land use/land cover change in Jordan's Irbid governorate, 1984–2018, and predicts future land use/land cover for 2030 and 2050 using a cellular automata-Markov model. The results inform planners and decision makers of past and current spatial dynamics of land use/land cover change and predicted urban expansion, for a better understanding and successful planning. Satellite images of Landsat 5-thematic mapper and Landsat 8 operational land imager for the years 1984, 1994, 2004, 2015 and 2018 were used to explore the characteristics of land use/land cover for this study. The results indicate that the built-up area expanded by 386.9% during the study period and predict further expansion by 19.5% and 64.6% from 2015 to 2030 and 2050 respectively. The areas around the central and eastern parts of the governorate are predicted to have significant expansion of the built-up area by these dates, which should be taken into consideration in future plans. Land use/land cover change and urban expansion in Irbid are primarily caused by the high rate of population growth rate as a direct result of receiving large numbers of immigrants from Syria and Palestine in addition to the natural increase of population and other socio-economic changes.

DOI: 10.22034/gjesm.2020.02.07

NUMBER OF REFERENCES	NUMBER OF FIGURES	NUMBER OF TABLES
36	5	9

*Corresponding Author:
Email: *h.khawaldah@ju.edu.jo*
Phone: +962772456053
Fax: +962-6-5300258

Note: Discussion period for this manuscript open until July 1, 2020 on GJESM website at the "Show Article.

INTRODUCTION

Research into land use and land cover (LULC) change is basic to an understanding of global change. Understanding LULC change dynamics and the factors responsible for such change are vital for modelling future changes to support sustainable and robust policy decisions and strategies (Munthali *et al.,* 2019). The whole world is experiencing rapid urban population growth (Ridd and Hipple, 2006; Yuan *et al.,* 2015; Khawaldah, 2016), and urbanization is one of the most evident global changes. Recently, the process of LULC change on local and regional scales has also become of interest to researchers, who believe that analyzing spatial patterns reveals the link between human activity and land use change (Meyer and Turner 1992; Han *et al.,* 2015). Population growth and urbanization lead to inward urban growth (intensification) and outward urban growth (sprawl) as well as a variety of socio-economic and urban-related environmental issues (Sexton *et al.,* 2013). Changes in LULC have significant impacts on both human systems and natural ecosystems (Munthali and Murayama, 2011; Khawaldah, 2016), of concern to planners, hydrologists, government agencies, ecologists, and so on. Nowadays, LULC change can be effectively monitored and detected using geographic information systems (GIS) and remote sensing (RS) technologies. Since the 1980s, remote sensing image data has been widely used in LULC data acquisition, spatial and temporal process expression, and model analysis and simulation (Yuan *et al.,* 2015). LULC models are powerful and trustworthy tools that help in analyzing LULC dynamic change and evaluating land use policy. Model analysis and LULC spatial patterns simulations reveal the driving forces that affect LULC, which can be used to predict future LULC change (Han *et al.,* 2015; Gillanders *et al.,* 2008). Many methods are used to model LULC dynamic change and simulation, including Cellular Automata (CA) (He *et al.,* 2005), the Clue-s model (Verburg and Overmars, 2007), the Markov model (Guan *et al.,* 2008) and the CA-Markov model (Khawaldah, 2016; Wang *et al.,* 2014). According to previous studies, LULC models can be classified into three categories: empirical-statistical models such as regression models, which ignore social factors (Bin and Tao, 2010); spatially explicit models such as Cellular Automata and Markov models, used to determine patterns of LULC change and to predict future changes, although it is still difficult to simulate the effect of human activities on LULC change (de Noronha Vaz *et al.,* 2013; Khawaldah, 2016); and agent-based models that simulate LULC change by considering individual agents, although only in simplified landscapes (Parker *et al.,* 2003; Han *et al.,* 2015). Verburg *et al.* (2008) noted that "no single model is capable of considering all of the processes of LULC change at different scales", despite the attempts to link biophysical and socio-economic data in LULC simulations (Veldkamp *et al.,* 2001; Alshalabi *et al.,* 2013). The Markov model is widely used to simulate and predict LULC change, representing the direction of change and offering a framework for examining future land use demand (Jiansheng *et al.,* 2012). Nevertheless, traditional models are inadequate in providing spatial analysis, with difficulty in allocating predicted land requirements in geographical space (Han *et al.,* 2015). The CA-Markov model, however, has strong dynamic simulation ability to present spatial and temporal changes. It combines the advantages of Markov and CA models in space and time series prediction and can be applied in LULC change simulation (Yuan *et al.,* 2015). Irbid city, the capital of the governorate and the second largest metropolitan area in Jordan after Amman, is undergoing rapid urbanization and currently has the highest population density in the country (Department of Statistics, 2019). This urban growth is the result of natural population increase and migration from the bordering countries and other governorates in Jordan. The Irbid governorate was therefore selected as a case study. The unplanned urban expansion has led to many problems, and predictions of future urban expansion are vital for urban planning. Simulation of future LULC will provide decision makers and planners with an indication of the direction of urban expansion and growth rates, essential in estimating the requirements for public services and infrastructure. The aim of this study is therefore to simulate and predict future LULC change dynamics in Irbid governorate using GIS and RS data from 1984 to 2018 to propose a map of LULC for the years 2030 and 2050. The objectives of this study can be summarized as: 1) To explore and analyze LULC change dynamics of Irbid from 1984 to 2018; 2) To simulate and predict the future LULC in Irbid for 2030 and 2050 with a focus on development of the built-up area using a Markov model. The study was carried out in Irbid governorate in Jordan during 2019.

MATERIALS AND METHODS

Study area

Irbid governorate, the second largest by population in Jordan and the first in terms of population density, has an area of 1,572 km^2 accounting for 1.8% of the Jordan's total area (Fig. 1). The population was approximately 1,911,600 in 2018, accounting for 18.5% of the country with a population density of 1,216.2 person/km^2 (Department of Statistics, 2019; Odeh *et al.,* 2019), and is one of the most developed and urbanized regions of Jordan (Awawdeh and Nawafleh, 2008; Al-Kofahi *et al.,* 2018). It was selected as a case study for its high rate of population growth (0.072% for the period 1984-2018) and urbanization over the last five decades. The population growth rate of Irbid governorate was calculated using the exponential equation (Vandermeer, 2010). The governorate is located in the extreme north-west of Jordan, about 80 kilometers north of Amman, between latitude 32.377 N and 32.745 N and longitude 35.547 E and 36.099 E. Irbid has a Mediterranean climate with an average rainfall of 454.5 mm annually for the period 1985-2014 (JMD, 2019). The elevation within the governorate ranges from 150 meters below sea level to 1,000 meters above (Margane *et al.,* 1999). The variety of LULC types, including agriculture, make it appropriate for detecting and simulating change over the years 1984 to 2050. Fertile plains occupy a large percentage of the study area and of the total area of plains in Jordan. Today, its historic function as the nation's bread basket is being overcome by urban uses (Awawdeh *et al.,* 2019). In 1884, Irbid was a small village of around 130 households with fewer than 700 people. However, the population increased to about 2,500 in 1922, out of Jordan's 225,000, and the built-up area did not exceed 210,000 square meters. By 1946, the population had risen to some 7,000. This population growth and commercial development extended the urban area (Tarrad, 2014). Commercial relations between northern Jordan and Damascus contributed to this increase. In addition to the natural increase in population, Irbid received the first wave of Palestinian refugees from the Arab-Israeli war of 1948. The first camp to accommodate refugees in the study area was established in 1951, covering 0.24 km^2 and inhabited by 4,000 refugees according to the United Nations Relief and Work Agency (UNRWA) (UNRWA, 2019). According to the census data, the population of Irbid reached 23,157 in 1952, rising to 44,685 in 1961 (Department of Statistics, 2019). The second wave of migration from Palestine to Jordan happened after the Arab-Israeli war of 1967, with

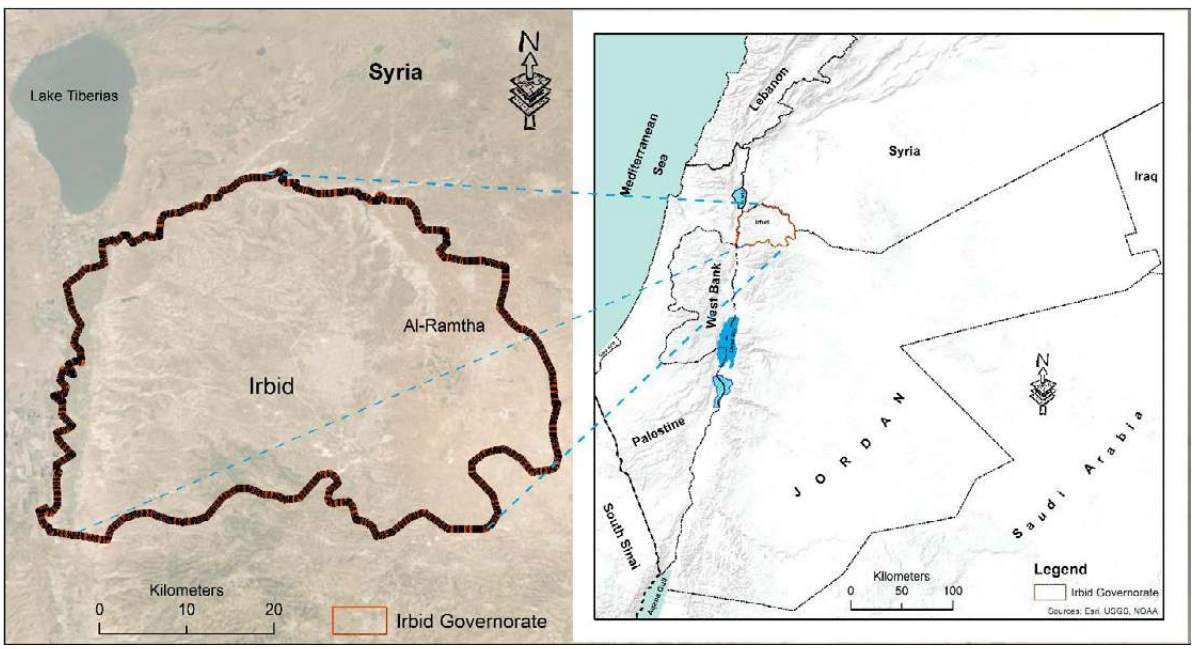

Fig. 1: Geographic location of the study area in Irbid governorate, Jordan

more than 700,000 people, most of whom settled in Amman, Zarqa and Irbid. The total number of people in the governorate was 113,548 in 1979, and the built-up area had expanded. The third wave of migrants to the city of Irbid happened after the Second Gulf War when Iraq entered Kuwait in 1990; 25,000 people arrived in the city of Irbid from Gulf countries. By 1994 the population of the whole governorate was over 750,000 and by 2004 over a million. With the recent wave of migration by Syrian refugees, from 2011, the governorate's population was approaching two million by the end of 2018 (Department of Statistics, 2019; Al-Kofahi *et al.,* 2018). This rapid population growth has led to several evolutionary stages for the city, with urbanization spreading outwards from the city centre into neighbouring villages. The built-up area in the governorate has also expanded for several reasons in addition to population growth: first, the development of large commercial and real-estate projects such as Al-Hassan Industrial Estate; and secondly the establishment of government educational institutions such as Yarmouk University in 1976 and Jordan University of Science and Technology in 1986. Together these have provided a large number of employment opportunities. Thus, the demand for land for urban use in a traditionally agricultural governorate has increased dramatically.

Data

Satellite images from Landsat 5 Thematic Mapper (TM) and Landsat 8 Operational Land Imager (OLI)/Terra were acquired from the United States Geological Survey (USGS) website. Cloud-free images from March and April were selected to represent the LULC for 1984, 1994, 2004, 2015 and 2018.

Image processing

Different pre-processing techniques were applied using ArcGIS 10.6 and ENVI classic 5.3 software to prepare the Landsat TM and OLI images for mapping the LULC changes. The image pre-processing techniques include: layer stacking; mosaicking; and subsetting or clipping to the borders of the study area. After that, the images were radio-metrically corrected using the atmospheric correction function. The images were then geometrically corrected using 40 Ground Control Points (GCPs) at road junctions based on a Global Positioning System (GPS) device with ±3-meter accuracy. A third-order transformation model was applied to correct different images by minimizing Root Mean Square Error (RMSE), and then the images were clipped to the borders of the study area. This was done through rectifying the image data set, where the cubic convolution "third-order transformation" provides an overall resampled image that is closest statistically to the original image and is also useful for resampling when the scale is changing radically. Table 1 shows the Landsat 5-TM and Landsat 8-OLI multi-bands with different wavelengths.

The schematic diagram shown in Fig. 2 includes a detailed description of these steps and procedures (methodology).

Table 1: Specification of Landsat TM and OLI bands, wavelengths and acquisition date

Image specification				
Image type	Landsat 5-TM		Landsat 8-OLI	
Swath width (km)	185		185	
Spectral range (µm)	Blue band (0.45-0.52)		Blue band (0.452-0.512)	
	Green band (0.52-0.60)		Green band (0.533-0.590)	
	Red band (0.63-0.69)		Red band (0.636-0.673)	
	NIR band (0.76-0.90)		NIR band (0.851-0.879)	
Spatial resolution (m)	Visible & NIR	30	Visible and NIR	30
Acquisition date (Day/Month/Year)	Three images:- 15-04-1984, 11-04-1994, 21-03-2004		Two images: 05-04-2015, 13-04-2018	
Revisit time (day)	16		16	
Launch	01 March 1984		11 February 2013	

LULC mapping

In order to generate LULC maps for assessing recent changes, different GIS functions and image processing methods were employed. Medium resolution satellite images for 1984, 1994, 2004, 2015 and 2018 were used to produce the maps through an on-screen digitizing procedure. The digitizing technique followed in this research was conducted using different Landsat images overlaid by the study area shapefile, as background image digitizing. The LULC classification scheme (Table 2) comprised seven LULC classes, identified by codes, to prepare different LULC for simulating future land use (Memarian *et al.*, 2012).

LULC classes were digitized as polygons by enclosing urban areas within specific boundaries, followed by the other types listed in the table. Field surveys were carried out throughout the study with the aid of GPS to verify the results of the recent LULC map. The maps were used to generate the predicted future LULC for the area.

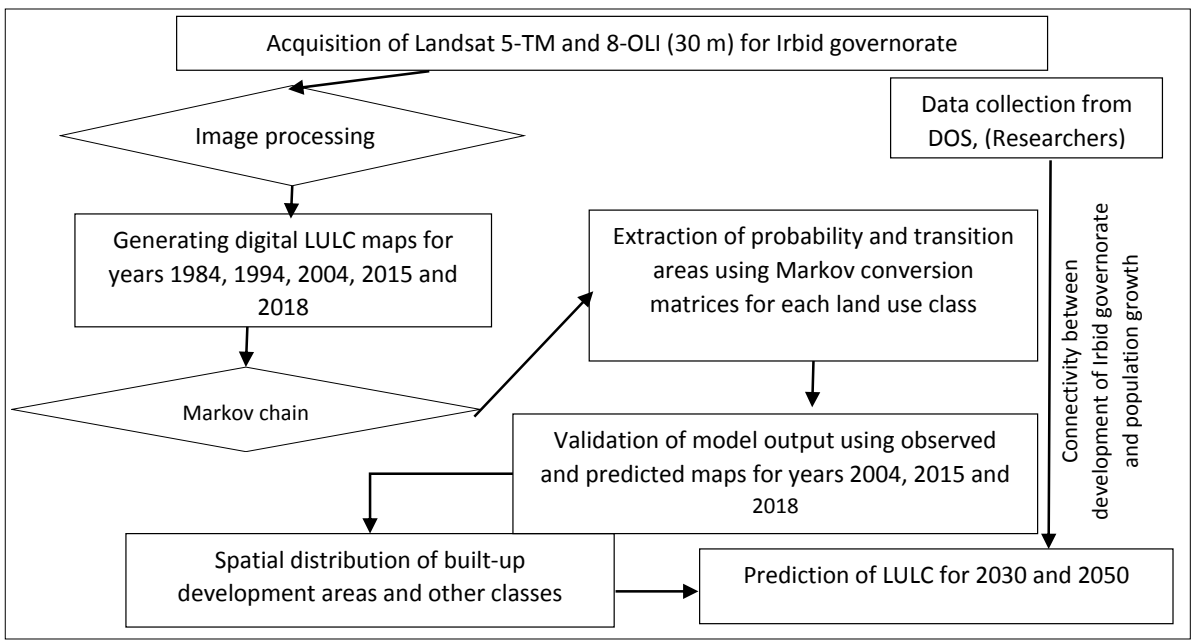

Fig. 2: The flow diagram of steps in simulating LULC changes

Table 2: Land use/land cover classification scheme used in the study

Class	Code	Description
Water bodies	1	Bodies of water including treated wastewater plants and dams.
Irrigated areas	2	Permanently irrigated lands; crop irrigated permanently or periodically, most of the crops that cannot be cultivated without an artificial water supply.
Rangeland	3	Open spaces with sparsely vegetated areas; heavily grazed open scrub and herbaceous rangeland.
Rainfed	4	Non-irrigated cereal crops in low rainfall areas.
Forest and trees	5	Continuous and discontinuous forested areas of conifers and oak. Also rainfed olive trees in high rainfall areas.
Built-up areas	6	Continuous and discontinuous urban areas; areas occupied by dwellings and areas occupied used by installations, buildings and factories (commercial and industrial), including their connected areas (associated lands, parking lots).
Bare land	7	Open spaces with no vegetation; bare rocks and limestone.

CA-Markov model

The CA-Markov model represents the integration of the standard Markov model and the Cellular Automata (CA). In the GIS environment, the spatio-temporal raster data model was used to illustrate the changes in continuous data over time among LULC classes using transition probabilities, while the CA method was used to control spatial dynamics. The LULC maps were generated within a GIS environment, then the LULC were exported as tiff format and classified into eight classes using Clark Labs TerrSet IDRISI software. These classes are: class 0- Background; class 1- Water bodies; class 2- Irrigated areas; class 3- Rangeland; class 4- Rainfed; class 5- Forest and trees; class 6 - Built-up areas; and class 7- Bare land. The land change modeler was then used to produce the predicted LULC map based on both the earlier LULC map and later LULC map. The transition areas and probability matrices of transition areas were generated using Clark Labs TerrSet IDRISI software (Eastman, 2016), with two techniques to produce the 2030 and 2050 predictions. The first analyzed the estimated LULC based on old and new maps of LULC to produce transition probability matrix records, which express the probability of each LULC class changing to another class. Second, the CA-Markov model was used to predict changes in the LULC classes for 2030 and 2050. This was performed using two LULC maps, which were produced from satellite images. The model was applied based on the number of random processes, **X** (t), for any moment in time, $t1 < t2 < \cdots < t_n < t_{n+1}$; thus, the random process will satisfy Eq. 1 (Singh *et al.,* 2015).

$$FX\,(X(tn+1) \le xn+1 \,|\, X(tn)) = xn,\ X(tn-1) = xn-1,..,\ X(t1) = FX\,(X(tn+1) \le xn+1 \,|\, X(tn)) = xn \quad (1)$$

Where, t_n is the present time and t_{n+1} denotes time points in the future; $t_1, t_2, \cdots, t_{n-1}$ represent time moments in the past. According to the present data, the future is independent of the past. In other words, the future random process depends neither on where it is now nor on where it was. If the Markov chain is expressed by X[k], and xn is a set of N states {x1, x2, x3, ⋯ xn}, then the probability of transition from state i to state j in one time instant is as Eq. 2.

$$P\,i,j\ \ Pr\,(X[k+1] = j \,|\, X[k] = i) \quad (2)$$

Validation of LULC changes and urban expansion

Validation is necessary in estimating development in any predictive change model, and is employed to calculate specialized Kappa indices (K_{no}, $K_{location}$, $K_{standard}$) that discriminate between errors of quantity and errors of location between two qualitative maps (Table 3). In this study, the validation technique was used to confirm the extent of congruence and difference between observed (actual) land use and predicted land use for the same year. Kappa statistics were used to reflect the simulation accuracy of the model based on the spatial pattern of observed and simulated LULC maps. The validation method was computed as Eq. 3 (Pontius and Millones, 2011):

$$Kappa = (p_o - p_c)/(1 - p_c) \qquad p_o = n/N \ ,\ p_c = 1/A \quad (3)$$

Where, P_o is the percent of actual LULC (digitized), P_c is the expected LULC simulation in stochastic cases, N is the total number of raster pixels in the LULC pattern, n is the number of raster of correct analogue, and A is the number of LULC types. The result is usually between 0 and 1. A value of Kappa below 0.4 indicates less precision and less consistency; when 0.4 ≤ Kappa ≤ 0.75 the accuracy is moderate; and when Kappa is greater than 0.75, there are small differences and a high level of consistency between the two LULC maps (Wu *et al.,* 2008; Qiu and Lu, 2018), (Table 3).

RESULTS AND DISCUSSION

Analysis of LULC changes

Analysis of the LULC maps for 1984, 1994, 2004, 2015 and 2018 reflects the changes in the balance

Table 3: Kappa indices definitions

Kappa Index	Definitions of the Kappa index of agreement
K_{no}	Measure of the overall proportion correctly classified versus the expected proportion correctly classified.
$K_{location}$	Measure of the spatial accuracy due to correct assignment of values.
$K_{standard}$	The proportion assigned correctly versus the proportion that is correct by chance.

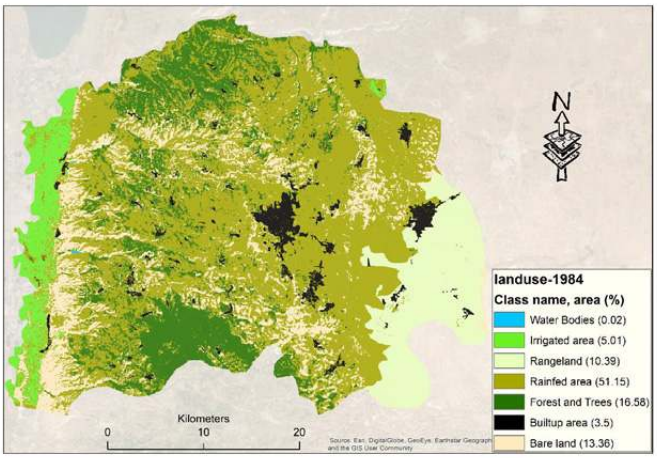

Fig. 3a: Land use in Irbid governorate in 1984

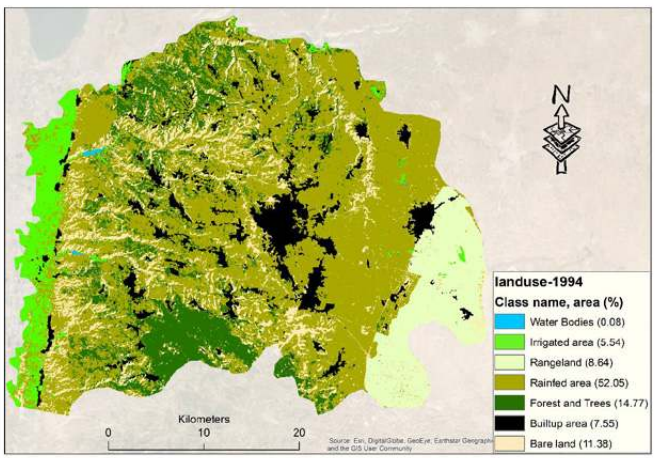

Fig. 3b: Land use in Irbid governorate in 1994

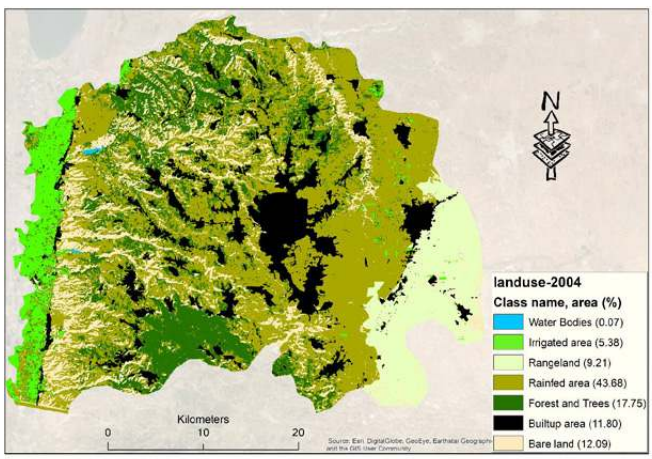

Fig. 3c: Land use in Irbid governorate in 2004

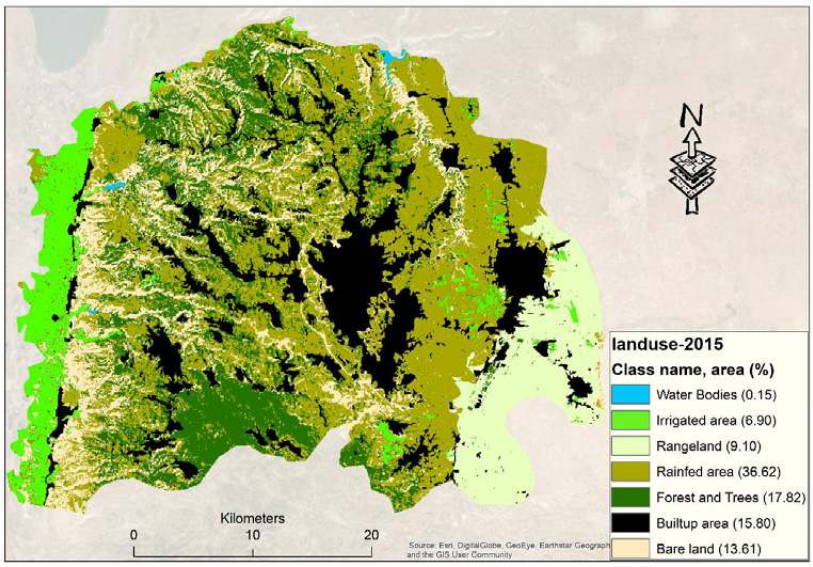

Fig. 3d: Land use in Irbid governorate in 2015

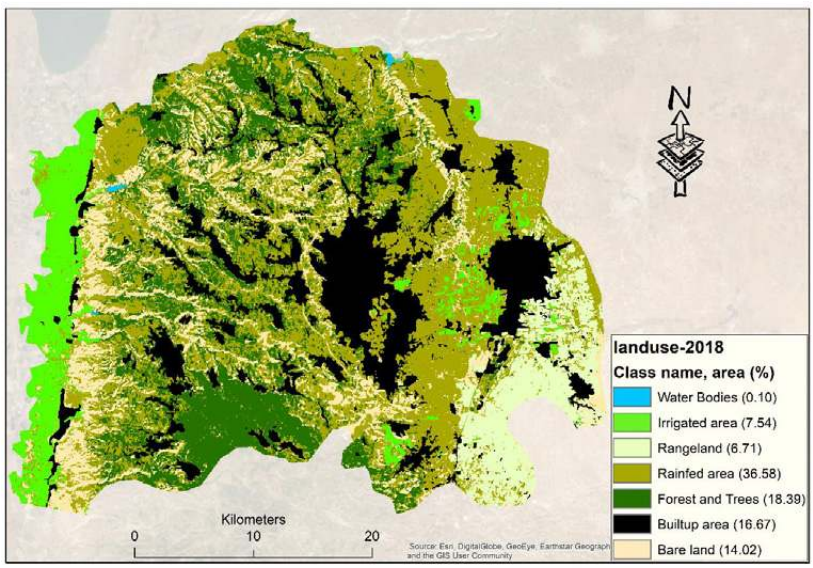

Fig. 3e: Land use in Irbid governorate in 2018

of the natural environment and human activity, with different patterns for each class in various parts of the governorate (Fig. 3a-e).

The western areas, which receive high rainfall, are mainly used for cultivating rainfed wheat, barley and olives. Most of the arid and semi-arid areas in the eastern parts are rangelands with little vegetation (Abu-Zanat *et al.,* 2004). Built-up areas have steadily increased, with urban growth occurring mainly in Irbid city, Ramtha and some other villages. The area under forest and trees has increased slightly as many are now protected under national conservation programs, while others are owned by local people and presented as agricultural tenure. Irrigated areas increased by 50.5% especially in the eastern part of the governorate because of shifts in agricultural type

Table 4: Correlation matrix (Pearson) (r) and (p-values) of LULC in the study area (1984-2050)

Variables	Water bodies		Irrigated area		Rangeland		Rainfed		Forest and trees		Built-up area		Bare land	
	r	p-value	r	p-value	r	p-value	r	p-value	r	p-value	r	p-value	r	p-value
Water bodies	**1**	**0**	0.600	0.155	0.404	0.369	0.692	0.085	0.334	0.464	0.674	0.097	0.253	0.584
Irrigated area	0.600	0.155	**1**	**0**	**-0.915**	**0.004**	**-0.878**	**0.009**	0.676	0.095	**0.814**	**0.026**	**0.771**	**0.043**
Rangeland	0.404	0.369	**-0.915**	**0.004**	**1**	**0**	**0.799**	**0.031**	0.482	0.274	**-0.829**	**0.021**	0.558	0.193
Rainfed	0.692	0.085	**-0.878**	**0.009**	**0.799**	**0.031**	**1**	**0**	0.662	0.105	**-0.958**	**0.001**	0.661	0.106
Forest and trees	0.334	0.464	0.676	0.095	0.482	0.274	0.662	0.105	**1**	**0**	0.447	0.314	**0.819**	**0.024**
Built-up area	0.674	0.097	**0.814**	**0.026**	**-0.829**	**0.021**	**-0.958**	**0.001**	0.447	0.314	**1**	**0**	0.457	0.302
Bare land	0.253	0.584	**0.771**	**0.043**	0.558	0.193	0.661	0.106	**0.819**	**0.024**	0.457	0.302	**1**	**0**

*Values in bold are different from 0 with a significance level alpha=0.05

Table 5: Establishment date and storage capacity of the study area dams

Dam	Establish date	Storage capacity (mcm)
Ziglab	1965	4
Wadi Arab	1986	20
Al Wahda	2004	115

Table 6a: Probability of transition class for LULC 1984-1994 (round one)

LULC 1984/1994	Water bodies	Irrigated area	Rangeland	Rainfed area	Forest and trees	Built-up area	Bare land	Percent
Water bodies	60.58	0.76	0	38.28	0.38	0	0	100
Irrigated area	0	71.65	0	25.21	0.52	1.5	1.12	100
Rangeland	0	0.85	66.41	24.17	0.56	1.15	6.86	100
Rainfed area	0.06	2.55	1.27	67.6	9.7	8.27	10.53	100
Forest and trees	0.15	2.15	0.01	31.88	53.98	3.91	7.92	100
Built-up area	0	1.35	1.1	10.36	1.26	83.1	2.82	100
Bare land	0.2	1.27	0.69	44.17	3.05	7.18	43.44	100

from rainfed to irrigated crops, an adaptation to the gradual decrease in annual rainfall over the last three decades. The correlation matrix of LULC in Table 4 shows that the built-up area is significantly correlated positively with irrigated areas and negatively with rangeland and rainfed areas. The irrigated area is negatively correlated with rangeland and rainfed areas.

The Ministry of Water and Irrigation (MWI) carried out different projects in Irbid governorate to increase the amount of stored rain water by the construction of dams, such as the Ziglab, Wadi Arab and Al Wahda dams; the area of water bodies thus gradually increased (Table 5). The quantity of stored rainfall water in these dams changes from year to year according to the amount and frequency of rainfall in the winter season.

Most of the rainfed area in the governorate is used for barley and wheat for flour. Rangelands in the eastern part constitute 6.7% of the area. In this zone, barley is cultivated for straw to support grazing herds of sheep. The non-cultivated areas are also heavily grazed and susceptible to soil erosion (Al-Bakri *et al.,* 2012).

Future simulation for LULC changes in 2030 and 2050

The LULC maps derived from the satellite images

Table 6b: Transition area of each class for 1984-1994 (round one)

LULC 1984/1994	Water bodies	Irrigated area	Rangeland	Rainfed area	Forest and trees	Built-up area	Bare land	Total cell
Water bodies	793	10	0	501	5	0	0	1309
Irrigated area	0	66938	0	23549	487	1402	1043	93419
Rangeland	0	1229	96580	35142	821	1672	9976	145420
Rainfed area	535	22560	11206	597003	85704	73074	93024	883106
Forest and trees	362	5124	30	75930	128575	9315	18869	238205
Built-up area	0	1728	1402	13222	1614	106032	3603	127601
Bare land	389	2524	1380	88069	6082	14315	86608	199367
Total cell	2079	100113	110598	833416	223288	205810	213123	1688427
changing trend	770	6694	-34822	-49690	-14917	78209	13756	

Table 6c: Probability of transition class for LULC 1994-2004 (round two)

LULC 1994/2004	Water bodies	Irrigated area	Rangeland	Rainfed area	Forest and trees	Built-up area	Bare land	Percent
Water bodies	**73.6**	0	2.47	14.18	3.35	5.73	0.67	100
Irrigated area	0.04	**67.15**	1.67	9.36	18.86	1.33	1.58	100
Rangeland	0	0.97	**75.49**	7.94	0.03	6.11	9.47	100
Rainfed area	0.01	2.07	3.39	**57.52**	17.41	9.54	10.05	100
Forest and trees	0.01	0.38	0.23	26.63	**58.74**	6.25	7.76	100
Built-up area	0	2.1	0.52	11.93	5.04	**75.15**	5.26	100
Bare land	0.01	0.36	1.74	29.36	10.33	8.73	**49.48**	100

Table 6d: Transition area of each class for 1994-2004 (round two)

LULC 1994/2004	Water bodies	Irrigated area	Rangeland	Rainfed area	Forest and trees	Built-up area	Bare land	Total cell
Water bodies	919	0	31	177	42	72	8	1249
Irrigated area	39	61057	1523	8514	17145	1210	1433	90921
Rangeland	0	1500	117072	12311	40	9478	14684	155085
Rainfed area	58	15197	24902	422238	127794	70056	73769	734014
Forest and trees	34	1154	681	80429	177389	18865	23421	301973
Built-up area	0	4179	1042	23759	10047	149689	10473	199189
Bare land	12	743	3575	60489	21271	17986	101915	205991
Total cell	1062	83830	148826	607917	353728	267356	225703	1688422
changing trend	-187	-7091	-6259	-126097	51755	68167	19712	

and the CA-Markov model were used to simulate changes for the years 2030 and 2050. According to the transition probability matrices (as shown in Table 6a to h), the results for the different periods show the probability of each class (n) in the LULC maps changing in the next period (t + n).

Accordingly, the LULC change in directions from one class to another was calculated using the Markov model (see the transition probability matrices in Table 6a to h). Negative trend values were observed for the rangeland, rainfed area, bare land, forest and trees classes during the period 1984 to 2018. This means that these areas changed mainly to built-up areas, irrigated areas and water bodies. In the tables, the bold values along the diagonal indicate the probability of a LULC class not changing from time t_0 to time t ($t > t_0$), while the cross diagonal shows the probability that one LULC experiences a change

Table 6e: Probability of transition class for LULC 2004-2018 (round three)

LULC 2004/2018	Water bodies	Irrigated area	Rangeland	Rainfed area	Forest and trees	Built-up area	Bare land	Percent
Water bodies	**59.24**	1.26	0	7.69	26.59	0	5.22	100
Irrigated area	0	**78.43**	0.14	10.06	4.02	5.66	1.7	100
Rangeland	0.01	1.45	**60**	25.07	0.63	8.96	3.88	100
Rainfed area	0.04	4.2	0.92	**58.92**	13.1	11.4	11.42	100
Forest and trees	0.2	5.13	0	24.12	**60.11**	6.53	3.91	100
Built-up area	0.03	0.8	0.13	10.77	7.31	**76.2**	4.76	100
Bare land	0.03	1.35	2.02	16.37	12.61	4.85	**62.78**	100

Table 6f: Transition area of each class for 2004-2018 (round three)

LULC 2004/2018	Water bodies	Irrigated area	Rangeland	Rainfed area	Forest and trees	Built-up area	Bare land	Total cell
Water bodies	983	21	0	128	441	0	87	1660
Irrigated area	0	99675	173	12781	5111	7197	2156	127093
Rangeland	16	1639	67602	28246	705	10098	4372	112678
Rainfed area	235	25819	5672	361930	80478	70015	70164	614313
Forest and trees	634	16033	0	75412	187931	20416	12237	312663
Built-up area	86	2269	372	30680	20845	217173	13574	284999
Bare land	69	3180	4734	38441	29605	11386	147428	234843
Total cell	2023	148636	78553	547618	325116	336285	250018	1688249
changing trend	363	21543	-34125	-66695	12453	51286	15175	

Table 6g: Probability of transition class for LULC 1984-2018 (total round)

LULC 1984/2018	Water bodies	Irrigated area	Rangeland	Rainfed area	Forest and trees	Built-up area	Bare land	Percent
Water bodies	**37.28**	3.8	0	19.26	26.8	0	12.86	100
Irrigated area	0	**79.12**	0	12.85	0.17	4.53	3.33	100
Rangeland	0	1.61	**52.71**	24.7	0.97	15.86	4.16	100
Rainfed area	0.04	4.96	0.93	**47.44**	16.71	19.42	10.5	100
Forest and trees	0.4	0.38	0	26.26	**53.25**	11.86	7.85	100
Built-up area	0.41	2.02	0.14	6.64	3.1	**83.23**	4.46	100
Bare land	0.15	4.05	0	24.17	7.73	13.37	**50.53**	100

Table 6h: Transition area of each class for 1984-2018 (total round)

LULC 1984/2018	Water bodies	Irrigated area	Rangeland	Rainfed area	Forest and trees	Built-up area	Bare land	Total cell
Water bodies	619	63	0	320	445	0	213	1660
Irrigated area	0	100551	0	16333	213	5755	4228	127080
Rangeland	0	1813	59379	27824	1090	17864	4687	112657
Rainfed area	217	30474	5714	291352	102593	119283	64500	614133
Forest and trees	1236	1200	0	82078	166462	37073	24551	312600
Built-up area	1162	5769	401	18919	8832	237175	12715	284973
Bare land	346	9521	0	56756	18151	31389	118653	234816
Total cell	3580	149391	65494	493582	297786	448539	229547	1687919
changing trend	1920	22311	-47163	-120551	-14814	163566	-5269	

Note: one cell is equal to 900 m^2

from one type to another. The results also reveal that during the period 1984 to 2018, different LULC types exhibited various dynamic conditions. The built-up and irrigated area classes are the most stable, with transition probabilities exceeding 79%. Water bodies, rangeland, rainfed area, bare land and forest and trees show less persistence, with probabilities of 37.3, 52.7, 47.4, 53.3 and 50.5 respectively (Table 6). As already explained, the governorate has received large numbers of migrants which, together with natural increase, contributes to the increase in the total size of the population, especially after Syrian refugees arrived from 2011. This process, however, resulted in less stability of the different LULC types.

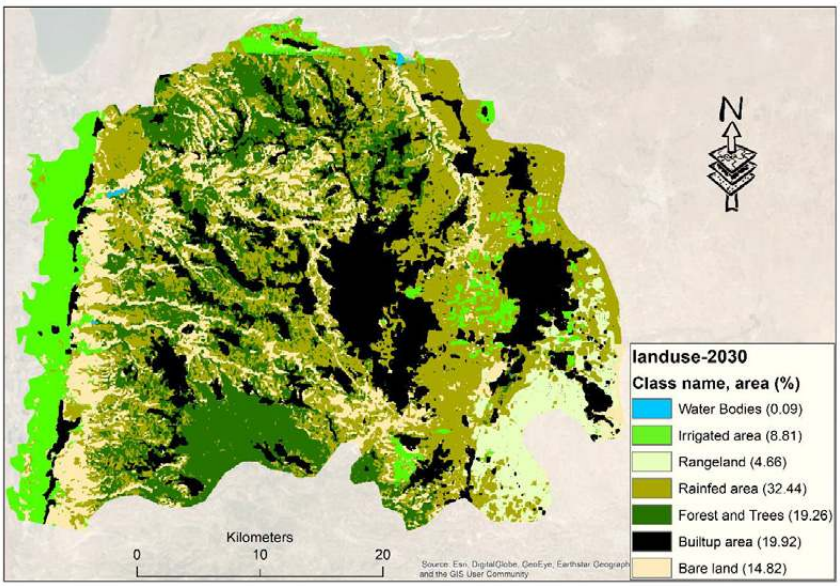

Fig. 4a: Predicted LULC changes in Irbid governorate for 2030

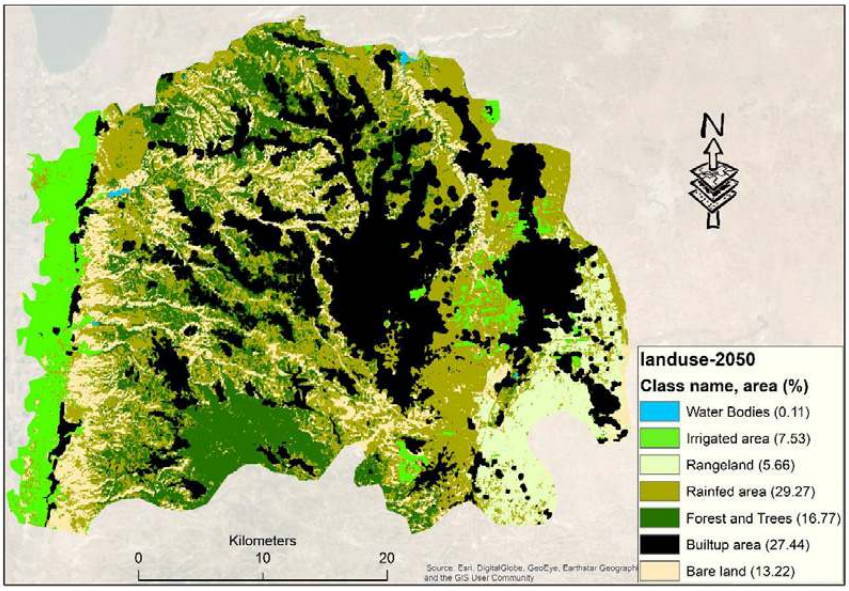

Fig. 4b: Predicted LULC changes in Irbid governorate for 2050

During the study period, most of the arable land was depleted by the expansion of the built-up areas, which means that urbanization consumed the largest quantities of rainfed, rangeland, and forest and trees areas (Table 6). In addition to the expansion of the built-up area, there was a conversion of rainfed areas to irrigated areas because of profit-oriented farming practices (Bani Hani, 2005). These factors together caused rainfed and rangeland to be the most dynamic types with the lowest transition persistence, 47% and 53% respectively. Built-up areas have the highest transition persistence, at 83%. After the successful simulation of LULC changes in 2004, 2015 and 2018, future changes for 2030 and 2050 were predicted using the LULC base map of 2018. The transition matrices for the period 2004 to 2018 were used to generate the LULC map of 2030, and the 1984 to 2018 ones to generate the LULC map of 2050, as shown in Fig. 4a-b.

The actual and predicted LULC maps in Figs. 3a-e and 4a-b show the trend of the spatio-temporal distributions of LULC changes for the six selected years 1984, 1994, 2004, 2018, 2030 and 2050. Tables 7 and 8 illustrate the total area coverage and percentage of gain and loss for each LULC type as the magnitude of change for the same periods. The results revealed that the spatial pattern changed during the study period. In 1984, rainfed, forest and trees, bare land, and rangeland were the dominant LULC types, accounting for 51.2%, 16.6%, 13.4%, and 10.4% of the total area respectively. The built-up area was largely limited to two areas: the central part of Irbid and Ramtha cities, representing only 3.5% of the study area. However, the built-up area expanded

Table 7: Summary of LULC changes during the period 1984 to 2018 in Irbid governorate.

LULC Type/years	Total area coverage (1520 km^2)													
	1984		1994		2004		2015		2018		2030		2050	
	No.	%	No.	%	No.	%	No.	%	No.	%	No.	%	No.	%
Water bodies	0.3	0.0	1.2	0.1	1.1	0.1	2.2	0.2	1.5	0.1	1.4	0.1	1.6	0.1
Irrigated area	76.1	5.0	84.3	5.5	81.8	5.4	105.0	6.9	114.6	7.5	133.9	8.8	114.4	7.5
Rangeland	157.9	10.4	131.3	8.6	140.0	9.2	138.3	9.1	101.9	6.7	70.8	4.7	86.0	5.7
Rainfed	777.6	51.2	791.3	52.1	664.1	43.7	556.7	36.6	556.0	36.6	493.1	32.4	445.0	29.3
Forest and trees	252.1	16.6	224.5	14.8	269.8	17.8	270.9	17.8	279.6	18.4	292.8	19.3	254.9	16.8
Built-up area	53.1	3.5	114.8	7.6	179.4	11.8	240.2	15.8	253.4	16.7	302.8	19.9	417.2	27.4
Bare land	203.1	13.4	173.0	11.4	183.9	12.1	206.8	13.6	213.2	14.0	225.2	14.8	200.9	13.2

Table 8: The percentage of gain/loss of area for LULC (1984 to 2050)

LULC Type/years	Gain/ loss (%) Between Different Times							
	1984 - 1994	1994 - 2004	2004 - 2015	2015 - 2018	2004 - 2018 (to produce 2030)	1984 - 2018 (to produce 2050)	2018 - 2030	2030 - 2050
Water bodies	262.7	-4.4	100.3	-33.6	33.0	361.3	-4.2	15.0
Irrigated area	10.7	-2.9	28.2	9.2	40.0	50.5	16.9	-14.6
Rangeland	-16.8	6.7	-1.2	-26.3	-27.2	-35.4	-30.5	21.4
Rainfed	1.8	-16.1	-16.2	-0.1	-16.3	-28.5	-11.3	-9.8
Forest and trees	-10.9	20.2	0.4	3.2	3.6	10.9	4.7	-12.9
Built-up area	116.0	56.2	33.9	5.5	41.3	376.9	19.5	37.8
Bare land	-14.8	6.3	12.5	3.1	16.0	5.0	5.7	-10.8

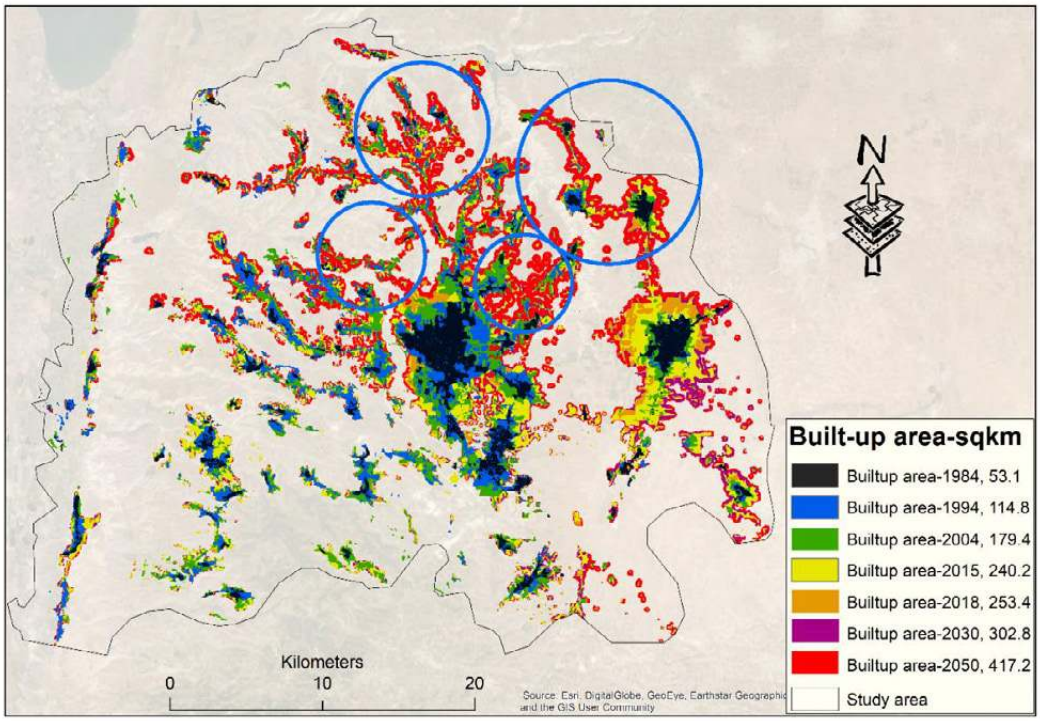

Fig. 5: Development of built-up area in Irbid governorate from 1984 to 2050

Table 9: Summary of Kappa indices for model validation

Maps used for simulation	Maps used for validation		Degree of compatibility	Kappa Index		
Observed LULC (Digitized)	Predicted LULC (Simulated)	Digitized LULC (Observed)	Validation of simulating CA-Markov (%)	K_{no}	$K_{location}$	$K_{standard}$
1984 - 1994	2004	2004	81.1	0.78	0.81	0.76
1994 - 2004	2015	2015	79.7	0.77	0.77	0.75
1984 - 2004	2018	2018	78.4	0.75	0.77	0.73

and increased by 377% between 1984 and 2018, accounting for 16.7% (Fig. 3a-e and Table 7), mainly at the expense of rangeland, rainfed, forest and trees cover types as shown in Table 6. During the period 1984 to 2018, water bodies increased from 0.3 km² to 1.5 km² due to the establishment of Al Wahda dam in 2004. Rangeland and rainfed types were negatively impacted by the increase in other types, showing a decrease in the same period. Even though the built-up and irrigated areas continue to increase more than other LULC types, the results indicate that the positive gain in expansion area was observed for the built-up area during the period 1984 to 2018, while between 2004 and 2018 the largest expansion was observed for the irrigated area, as compared to the earlier decades.

The general trend of built-up area changes in Irbid governorate reveals that the changes that occurred during the study period are expected to continue in 2030 and 2050. According to the predicted results, the spatio-temporal pattern of built-up area continues to expand and is expected to cover more than 19.9% of the total study area in 2030 and and 27.4% in 2050 (Fig. 4a-b and Tables 7 and 8). Additionally, the irrigated area will continue to increase due to high economic returns for this LULC type. The predicted results also indicate that the rainfed and rangeland classes will witness a decrease

in future, as shown in Table 7. Generally, these LULC types have been replaced by built-up and irrigated areas (Table 6). Therefore, the current and ongoing trends (gains and losses) have compressed those LULC classes with significant environmental value, which may result in dilapidation and devastation. Finally, the governate as an arid and semi-arid area (Farhan *et al.,* 2013) is highly sensitivity to adverse effects on environmental sustainability. Therefore, appropriate management for land use plans and utilization is needed, with emphasis on controlling the encroachment of built-up areas (residential, commercial and industrial) on rainfed area, rangeland, forest and trees. Fig. 5 shows the development of built-up area in the governorate from 1984 to 2050.

Validation of CA-Markov model results

A comparison of the LULC maps for the years 2004, 2015 and 2018 with the CA-Markov simulated map was made based on the Kappa statistics (Table 9). The results show good agreement with a high level of consistency and small differences between the predicted values and the observed values of the LULC types, with $K_{no,}$ $K_{location}$ and $K_{standard}$ above 0.75, 0.77 and 0.73 respectively. Thus, there are almost no or small quantification and location errors. On the other hand, Kappa indices of agreement were used to validate and confirm different changes that could happen in the LULC maps of 2030 and 2050. The results proved that the CA-Markov model is an effective tool to simulate and analyze different changes of LULC in 2030 and 2050. Thus, the model is considered reliable and trustworthy in simulating and predicting future LULC change. The LULC was generated using On-screen digitizing due to the heterogeneity features in the study area; so if different techniques are applied, such as supervised or unsupervised classification methods, the percentage of error will increase in this case. Thus, the On-screen digitizing method is the best method for reflecting the current feature (LULC) with an accuracy of more than 98% based on the ground resolution of Landsat and equal ± 30 meters. After that, LULC maps for the years 2004, 2015 and 2018 were simulated as shown in Table 9. These maps were compared with actual maps that were generated using GIS software. The Kappa index indicates that there is good agreement to produce the LULC maps of 2030 and 2050 with an accuracy level of approximately 80 %.

CONCLUSION

The study has examined LULC changes in Irbid governorate during the period 1984-2018 and simulated land use demand in the future using a CA-Markov model, which gives a better understanding of possible changes in LULC within the study area. The results indicate that with rapid urban growth, fertile plains were converted to built-up land by 21.4% with an area of 200.3 km², a trend that will become the main feature of LULC in the future. The changes are significant and clearly noticeable in four main zones, mainly in the north and northeast of the governorate. Results revealed that the built-up area expanded from only 53.1 km² in 1984 to 253.4 km² in 2018, an increase of 377%. This change in the built-up land is caused by the rapid population increase, with population growth rate at 0.072, resulting from immigration and internal migration. The irrigated area has also increased, with intensive use of land to meet the population demand. However, other LULC types decreased significantly during the same period, especially the rainfed and rangeland types which were converted to built-up area. These noticeable changes have altered the identity of the governorate from an agricultural region to an urban area. Urban sprawl is considered as a key indication that urban planning strategy should be given more attention. A simulation of future LULC was also demonstrated using a CA-Markov model for 2030 and 2050. The results revealed that built-up land will continue to increase and is expected to cover around 20% and 27% of the total study area in 2030 and 2050 respectively. Agricultural types such as rainfed and rangeland areas will be threatened. The implication of this study is the importance of considering these predicted changes. The city must plan for future infrastructure, road networks, and allocating locations for future services such as health centers, schools and public parks. At the same time, planning to control urban sprawl and protecting the remaining agricultural areas should be a priority for planners and decision makers for sustainable development. The CA-Markov model has proved to be a powerful tool for analyzing LULC dynamic change and predicting future scenarios.

AUTHOR CONTRIBUTIONS

H.A. Khawaldah contributed in this article by collecting data, conducting the preliminary analysis and writing the critical literature review section and manuscript draft; I. Farhan participated in mapping the land use and land cover change and participated in field survey and N.M. Alzboun participated in result validation and reviewed and edited the manuscript draft.

ACKNOWLEDGMENTS

The authors would like to thank the University of Jordan for providing a suitable environment in which to carry out this research, the Department of Statistics for supplying the necessary data, and USGS for making available the requested Landsat images.

CONFLICT OF INTERESTS

The author declares that there is no conflict of interests regarding the publication of this manuscript. In addition, the ethical issues, including plagiarism, informed consent, misconduct, data fabrication and/or falsification, double publication and/or submission, and redundancy have been fully observed by the authors.

ABBREVIATIONS

%	Percent
CA	Cellular automata
DoS	Department of Statistics
E	East
Eq.	Equation
Fig.	Figure
GIS	Geographic information system
GCP's	Ground Control Point's
GPS	Global Positioning System
km	Kilometer
km²	Square kilometer
LULC	Land Use and Land Cover
m	Meter
m²	Square meter
mcm	Million cubic meter
mm	Millimeter
µm	Micrometer
MWI	Ministry of Water and Irrigation
N	North
NIR	Near Infrared
OLI	Operational land imager
p-value	Probability value
RS	Remote sensing
TM	Thematic mapper
UNRWA	The United Nations Relief and Work Agency
USGS	United State Geological Survey

REFERENCES

Abu-Zanat, M.W.; Ruyle, G.B.; Abdel-Hamid, N.F., (2004). Increasing range production from fodder shrubs in low rainfall areas. J. Arid Environ., 59(2): 205-216 **(12 pages).**

Al-Kofahi, S. D.; Jamhawi, M. M.; Hajahjah, Z. A., (2018). Investigating the current status of geospatial data and urban growth indicators in Jordan and Irbid municipality: implications for urban and environmental planning. Environment, development and sustainability, 20(3): 1067-1083 **(17 pages).**

Al-shalabi, M.; Billa, L.; Pradhan, B.; Mansor, S.; Al-Sharif, A.A., (2013). Modelling urban growth evolution and land-use changes using GIS based cellular automata and SLEUTH models: the case of Sana'a metropolitan city, Yemen. Environ. Earth Sci., 70(1): 425-437 **(13 pages).**

Awawdeh, M.; Nawafleh, A., (2008). A GIS-based EPIK model for assessing aquifer vulnerability in Irbid Governorate, North Jordan. Jordan J. Civil Eng., 2(3): 267-278 **(12 pages).**

Awawdeh, M.; Jaradat, R.; Al Qudah, K.; Abu-Jaber, N.; Awawdeh, M., (2019). A GIS-based Hydrogeological and Geophysical Study for the Analysis of Potential Water Infiltration in the Upper Yarmouk River Basin, North Jordan. Jordan J. Earth Environ. Sci., 10 (3): 136-144 **(9 pages).**

Bani Hani, M., (2005). Management of irrigation water in Jordan. AARDO – International Workshop: Role of modern irrigation techniques in improving food security.

Bin, P.; Tao, P., (2010). Land use system dynamic modeling: literature review and future research direction in China. Progress Geogr., 29(9), 1060-1066 **(7 pages).**

de Noronha Vaz, E.; Walczynska, A.; Nijkamp, P., (2013). Regional challenges in tourist wetland systems: an integrated approach to the Ria Formosa in the Algarve, Portugal. Reg. Environ. Change, 13(1): 33-42 **(10 pages).**

Department of Statistics, (2019) Jordan Statistical Yearbook 2018, Amman, Jordan.

Al-Bakri, J., Saoub, H., Nickling, W., Suleiman, A., Salahat, M.,

Khresat, S., & Kandakji, T. (2012, October). Remote sensing indices for monitoring land degradation in a semiarid to arid basin in Jordan. In Earth Resources and Environmental Remote Sensing/GIS Applications III (Vol. 8538, p. 853810). International Society for Optics and Photonics **(10 pages).**

Eastman J.R., (2016). TerrSet Geospatial Monitoring and Modeling System - Clark University, Worcester. Source code 1987-2016 **(30 pages).**

Farhan, Y.; Zregat, D; Farhan, I. (2013). Spatial estimation of soil erosion risk using RUSLE approach, RS, and GIS techniques: a case study of Kufranja watershed, Northern Jordan J. Water Resour. Prot., 5(12): 1247 **(15 pages).**

Gillanders, S. N.; Coops, N. C.; Wulder, M.A.; Goodwin, N. R., (2008). Application of landsat satellite imagery to monitor land-cover changes at the Athabasca Oil Sands, Alberta, Canada. Can. Geogr, 52 (4), 466-485 **(20 pages).**

Guan, D.; Gao, W.; Watari, K.; Fukahori, H., (2008). Land use change of Kitakyushu based on landscape ecology and Markov model. J. Geog. Sci., 18(4): 455-468 **(24 pages).**

Han, H.; Yang, C.; Song, J., (2015). Scenario simulation and the prediction of land use and land cover change in Beijing, China. Sustainability. 7(4): 4260-4279 **(20 pages).**

He, C.; Pan, Y.; Shi, P.; Li, X.; Chen, J.; Li, Y.; Li, J., (2005). Developing land use scenario dynamics model by the integration of system dynamics model and cellular automata model. Sci. China Ser. D: Earth Sci., 48(11): 1979-1989 **(11 pages).**

Jiansheng, W.; Zhe, F.E.N.G.; Yang, G.A.O.; Xiulan, H.U.A.N.G.; Hongmeng, L.I.U.; Li, H.U.A.N.G., (2012). Recent progresses on the application and improvement of the CLUE-S model. Progress in Geography, (1): 3-10 **(8 pages).**

JMD, (2019). Climate information: rainfall averages. Jordan Meteorological Department. Amman, Jordan.

Khawaldah, H.A., (2016). A prediction of future land use/land cover in Amman area using GIS-based Markov Model and remote sensing. J. Geogr. Inf. Syst., 8(03): 412-427 **(16 pages).**

Khresat, S.A.; Rawajfih, Z.; Mohammad, M., (1998). Morphological, physical and chemical properties of selected soils in the arid and semi-arid region in north-western Jordan. J. Arid. Environ., 40(1): 15-25 **(11 pages).**

Margane, A.; Hobler, M.; Subah, A., (1999). Mapping of Groundwater Vulnerability and Hazards to Groundwater in the Irbid Area, N-Jordan. Z. Angew. Geol., 45(4): 175-187 **(13 pages).**

Memarian, H.; Balasundram, S.K.; Talib, J. B.; Sung, C.T.B.; Sood, A. M.; Abbaspour, K., (2012). Validation of CA-Markov for simulation of land use and cover change in the Langat Basin, Malaysia. J. Geogr. Inf. Syst., 4(6): 542-554 **(13 pages).**

Meyer, W.B.; Turner, B.L., (1992). Human population growth and global land-use/cover change. Ann. Rev. Ecol. Syst., 23(1): 39-61 **(23 pages).**

Munthali, M. G.; Davis, N.; Adeola, A.M.; Botai, J.O.; Kamwi, J. M.; Chisale, H.L.; Orimoogunje, O.O., (2019). Local Perception of Drivers of Land-Use and Land-Cover Change Dynamics across Dedza District, Central Malawi Region. Sustainability, 11(3): 832 **(25 pages).**

Munthali, K.G.; Murayama, Y., (2011). Land use/cover change detection and analysis for Dzalanyama forest reserve, Lilongwe, Malawi. Procedia- Soc. Behav. Sci., 21: 203-211 **(9 pages).**

Odeh, T.; Mohammad, A. H.; Hussein, H.; Ismail, M.; Almomani, T., (2019). Over-pumping of groundwater in Irbid governorate, northern Jordan: a conceptual model to analyze the effects of urbanization and agricultural activities on groundwater levels and salinity. Environ. Earth Sci., 78(1): 40: 1-12 **(12 pages).**

Parker, D.C.; Manson, S.M.; Janssen, M.A.; Hoffmann, M.J.; Deadman, P., (2003). Multi-agent systems for the simulation of land-use and land-cover change: a review. Annals Association Am. Geogr., 93(2): 314-337 **(24 pages).**

Pontius Jr, R.G.; Millones, M., (2011). Death to Kappa: birth of quantity disagreement and allocation disagreement for accuracy assessment. Int. J. Remote Sens., 32(15): 4407-4429 **(23 pages).**

Qiu, Y.; Lu, J., (2018). Dynamic simulation of Spartina alterniflora based on CA-Markov model--a case study of Xiangshan bay of Ningbo City, China. Aquat. Invasions, 13(2): 299–309 **(11 pages).**

Ridd, M.K.; Hipple, J.D., (2006). Remote Sensing of Human Settlements: Manual of Remote Sensing, 3rd Edition. American Society for Photogrammetry and Remote Sensing. ISBN 1-57083-077-0.

Sexton, J.O.; Song, X.; Huang, C.; Channan, S., (2013) Urban growth of the Washington, D.C.-Baltimore, MD metropolitan region from 1984 to 2010 by annual, landsat-based estimates of impervious cover. Remote Sens. Environ., 129: 42-53 **(12 pages).**

Singh, S. K.; Mustak, S.; Srivastava, P. K.; Szabó, S.; Islam, T., (2015). Predicting spatial and decadal LULC changes through cellular automata Markov chain models using earth observation datasets and geo-information. Environ. Process., 2(1), 61-78. **(18 pages).**

Tarrad, M., (2014). Urban Planning Response to Population Growth in Jordanian Cities (Irbid City as Case Study). Res. J. Appl. Sci. Eng. Technol., 7(20): 4275-4280 **(6 pages).**

UNRWA, (2019). Irbid camp. Jordan. The United Nations Relief and Work Agency

Vandermeer, J. (2010). How populations grow: the exponential and logistic equations. Nature Education Knowledge, 3(10): 15.

Veldkamp, A.; Verburg, P.H.; Kok, K.G.H.J.; De Koning, G.H.J.; Priess, J.; Bergsma, A.R., (2001). The need for scale sensitive approaches in spatially explicit land use change modeling. Environ. Model. Assess., 6(2): 111-121 **(11 pages).**

Verburg, P.H.; Eickhout, B.; van Meijl, H., (2008). A multi-scale, multi-model approach for analyzing the future dynamics of European land use. Ann. Region. Sci., 42(1): 57-77 **(21 pages).**

Verburg P.; Overmars K., (2007) Dynamic Simulation of Land-Use Change Trajectories with the Clue-S Model. In: Koomen E.; Stillwell J.; Bakema A.; Scholten H.J., (eds) Modelling Land-Use Change. The GeoJournal Library, vol 90. Springer, Dordrecht **(17 Pages).**

Wang, S.; Zhang, Z.; Wang, X., (2014). Land use change and prediction in the Baimahe Basin using GIS and CA-Markov model. In IOP conference series: Earth Environ. Sci., 17(1): 012074. IOP Publishing **(6 pages).**

Wu, X.Q.; Hu, Y.M.; He, H.S.; Bu, R.C., (2008). Accuracy evaluation and its application of SLEUTH urban growth model. Geomatics and Information Science of Wuhan University, 33(3): 293-296 **(4 pages).**

Yuan, T.; Yiping, X.; Lei, Z.; Danqing, L., (2015). Land use and cover change simulation and prediction in Hangzhou city based on CA-Markov model. International Proceedings of Chemical. Biol. Environ. Eng., 90: 108-113 **(6 pages).**

AUTHOR (S) BIOSKETCHES

Khawaldah, H.A., Ph.D., Associate Professor, Department of Geography, Faculty of Arts, The University of Jordan, Amman, Jordan.
Email: *h.khawaldah@ju.edu.jo*

Farhan, I., Ph.D., Instructor, Department of Geography, Faculty of Arts, The University of Jordan, Amman, Jordan.
Email: *ibmfrhan@yahoo.com*

Alzboun, N.M., Ph.D., Associate Professor, Department of Geography, Faculty of Arts, The University of Jordan, Amman, Jordan.
Email: *n.alzboun@ju.edu.jo*

HOW TO CITE THIS ARTICLE

Khawaldah, H.; Farhan, I.; Alzboun, N., (2020). Simulation and prediction of land use and land cover change in Irbid governorate in Jordan using GIS, remote sensing and CA-Markov model. Global J. Environ. Sci. Manage., 6(2): 215-232.

DOI: 10.22034/gjesm.2020.02.07

url: https://www.gjesm.net/article_37291.html